



## Complete flux jumping in nano-structured MgB<sub>2</sub> superconductors prepared by mechanical alloying

E. Yanmaz<sup>a,\*</sup>, B. Şavaşkan<sup>a</sup>, M. Başoğlu<sup>a</sup>, E. Taylan Koparan<sup>a</sup>, N.R. Dilley<sup>b</sup>, C.R.M. Grovenor<sup>c</sup>

<sup>a</sup> Department of Physics, Faculty of Arts & Sciences, Karadeniz Technical University, 61080 Trabzon, Turkey

<sup>b</sup> Quantum Design, Inc., 6325 Lusk Boulevard, San Diego, CA 92121, USA

<sup>c</sup> Department of Materials, University of Oxford, Parks Road, OX1 3PH, Oxford, UK

### ARTICLE INFO

#### Article history:

Received 12 November 2008

Received in revised form 8 February 2009

Accepted 10 February 2009

Available online 21 February 2009

#### Keywords:

MgB<sub>2</sub> superconductor

Mechanical alloying

Defects

Pinning centres

Critical current density

Flux jumping

### ABSTRACT

High density nano-crystalline MgB<sub>2</sub> bulk superconductors with induced pinning centres were prepared from elemental precursors by a sequence of ball milling, heat treatment, and final pressing. The XRD results revealed the main phase was MgB<sub>2</sub> with a minor component of MgO. The magnetic moment versus temperature indicated that the transition temperature of MgB<sub>2</sub> samples was around 34 K, which is less than the typical transition temperature of commercial powders and also the transition temperature strongly depended on the milling time. It is well known that introduction of defects, grain boundaries and impurities act as effective flux pinning centres in MgB<sub>2</sub> and results in increased critical current density,  $J_c$  and decreased the transition temperature,  $T_c$ . The magnetization measurements were performed using VSM at 10 K, 20 K and 30 K, and the  $M-H$  curves indicated a complete flux jump effect, which is a severe problem for the application of superconductors. It was determined that a noticeable amount of heating ( $\sim 0.3$  K jumps at 10 K) occurs at these jumps. In addition, it was found that the sweeping rate of magnetic field and the size of bulk sample are very effective to promote the flux jumping and whereas a low sweeping rate (12 Oe/s) avoids these “avalanches”, consistent with a kind of supercritical phenomenon: going slower allows the field gradients to stay close enough to equilibrium so that the avalanche effect is not triggered. In contrast, the sweeping rate of 100 Oe/s leads to numerous jumps.

© 2009 Elsevier B.V. All rights reserved.

### 1. Introduction

Since the discovery of superconductivity in MgB<sub>2</sub> [1], many efforts have been given to characterize the structure and physical properties. MgB<sub>2</sub> superconductors show important potentials for the applications if the material properties are improved [2]. It was reported that introduction of defects, grain boundaries and impurities act as effective flux pinning centres in MgB<sub>2</sub> and result in increased critical current density,  $J_c$ . These defects also affect the current flow or pairing interaction and often decrease the transition temperature,  $T_c$  [2,3].

Wang et al. [4] have succeeded to increase pinning centres by introducing disorder, such as, substitution of nanometer sized particles of Si, C, SiC. In addition, SiC addition leads to enhancement of  $J_c$  and  $H_{irr}$  while leaving the critical temperature  $T_c$  almost unchanged [3]. Fe has a very little effect on superconductivity because of very low solubility of Fe in MgB<sub>2</sub> structure. No significant reduction of critical temperature ( $T_c$ ) was found in Fe substituted specimens. The low solubility of Fe benefits the fabrica-

tion of MgB<sub>2</sub> wire, cable and tape using Fe tube [5]. It was indicated that the mechanical alloying is a well-established method to prepare metastable amorphous, quasicrystalline and nanocrystalline materials [6]. Mechanical alloying technique allows one to prepare materials at ambient temperature in a solid state reaction, which normally form only during heat treatment. Hence Mg loss due to evaporation will be avoided and oxidation of the constituents can be minimized [7,8].

In order to use superconductors for industrial applications, the superconductor must be able to carry a large current in the presence of a magnetic field in the range of 5–10 T. Type II superconductors appear appropriate because of their large upper critical field and of high currents being permitted to flow in the bulk material. But a flux jumping phenomena [9] have been a severe problem for the application of superconductors. In general case two types of flux jumps can be considered, namely, global and local flux jumps. A global flux jump involves vortices into motion in the entire volume of the sample. A local flux jump occurs in a small fraction of the sample volume. The first turn the superconductor to normal state and the second self terminates when the temperature is still less than the critical temperature [10]. The large flux jumps were observed experimentally in the YBa<sub>2</sub>Cu<sub>3</sub>O<sub>x</sub> [11], Bi<sub>2</sub>Sr<sub>2</sub>CaCu<sub>2</sub>O<sub>8</sub> [12] superconductors. Only small flux jump in MgB<sub>2</sub> created by dendritic

\* Corresponding author. Tel.: +90 462 377 2541; fax: +90 462 325 3195.

E-mail address: [yanmaz@ktu.edu.tr](mailto:yanmaz@ktu.edu.tr) (E. Yanmaz).

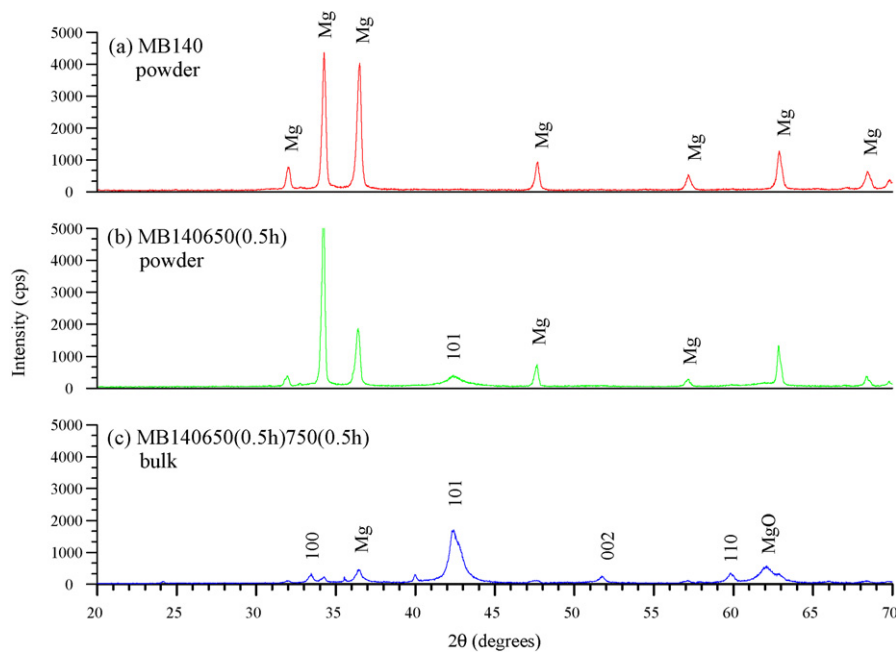


**Fig. 1.** X-ray patterns of (a) 140 h milled powders, (b) 140 h milled and reacted at 650° for 30 min and (c) 140 h milled, reacted at 650° for 30 min and sintered at 750 °C for 30 min.

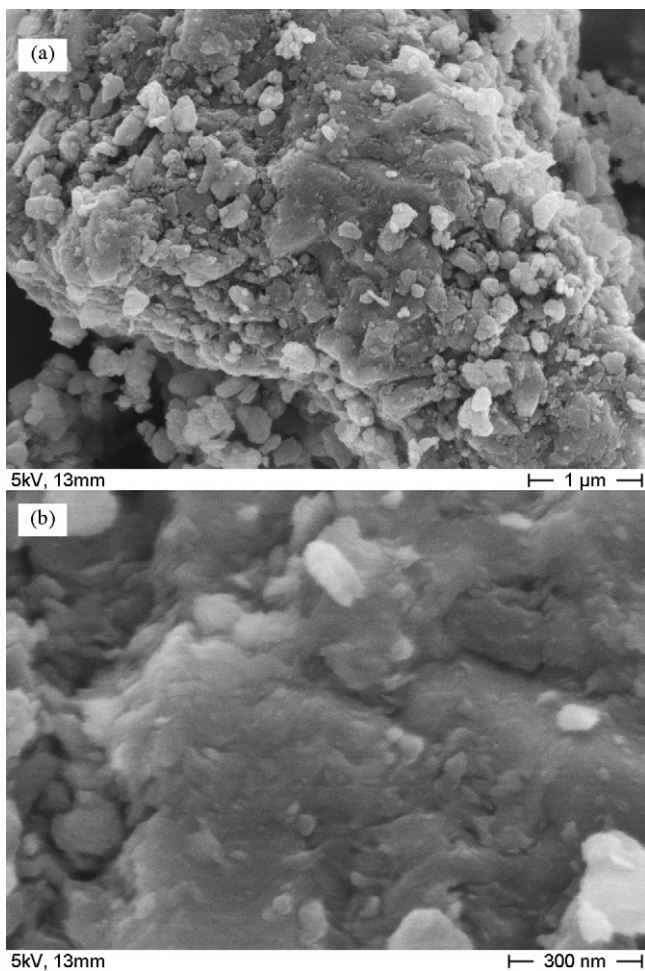


**Fig. 2.** SEM images of sample MGB140 powders at different magnifications.

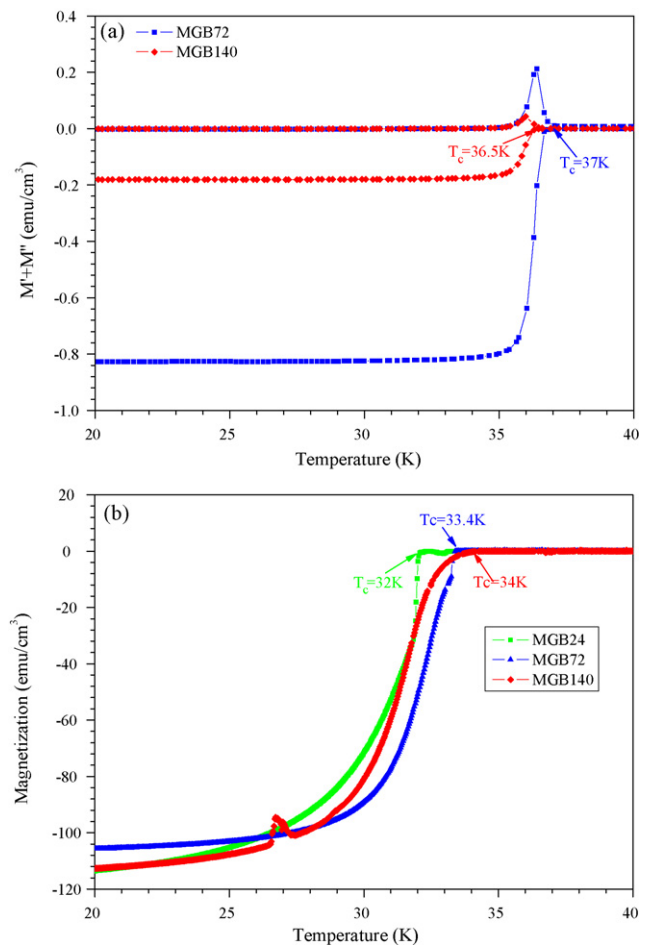


**Fig. 3.** (a) ac susceptibility in real ( $M'$ ) and imaginary ( $M''$ ) parts and (b) moment versus temperature curves for MgB<sub>2</sub> samples.

magnetic instability below 10 K were frequently observed in the low field region [13]. The complete flux jump in  $\text{MgB}_2$  was first time reported by Gumbel et al. [6].

Here, we present the structural and physical and magnetic properties of nano-sized  $\text{MgB}_2$  superconductor prepared by mechanical alloying process and a complete flux jump in  $\text{MgB}_2$  at 10 K was also described.

## 2. Experimental procedure

Nanocrystalline  $\text{MgB}_2$  powders were prepared by ball milling, starting with amorphous B (95% purity, 1  $\mu\text{m}$  grain size, Alfa Aesar) and grained Mg (99.8%,

250  $\mu\text{m}$ , Alfa Aesar) powders. The particle size of Mg powder used was 250  $\mu\text{m}$ . It was thought that the reaction of this powder with Boron could be difficult to form  $\text{MgB}_2$ . Therefore, an agate mortar and pastel as well as a 106  $\mu\text{m}$  mesh were put into nitrogen glove box. An appropriate amount of Mg powders were ground by hand and sieved to 106  $\mu\text{m}$ . Then, three of each 15 g mixture of Mg and B powders with stoichiometric ratio of  $\text{MgB}_2$  were put into the three plastic bottles containing YSZ balls (~3 mm in diameter) in a nitrogen glove box and were the lids strongly tightened. The ball to powder mass ratio was chosen to be 24:1. The bottles were milled for 24, 72, and 140 h respectively. The milled powders were then sintered in a special designed furnace (stainless steel closed volume) at 650 °C for 30 min and cooled to room temperature in argon atmosphere. Finally, the sintered powders were pressed at room temperature in air under the pressure of 6000 psi into pellet form diameter 15 mm and re-sintered at 700 °C for 30 min in argon atmosphere to

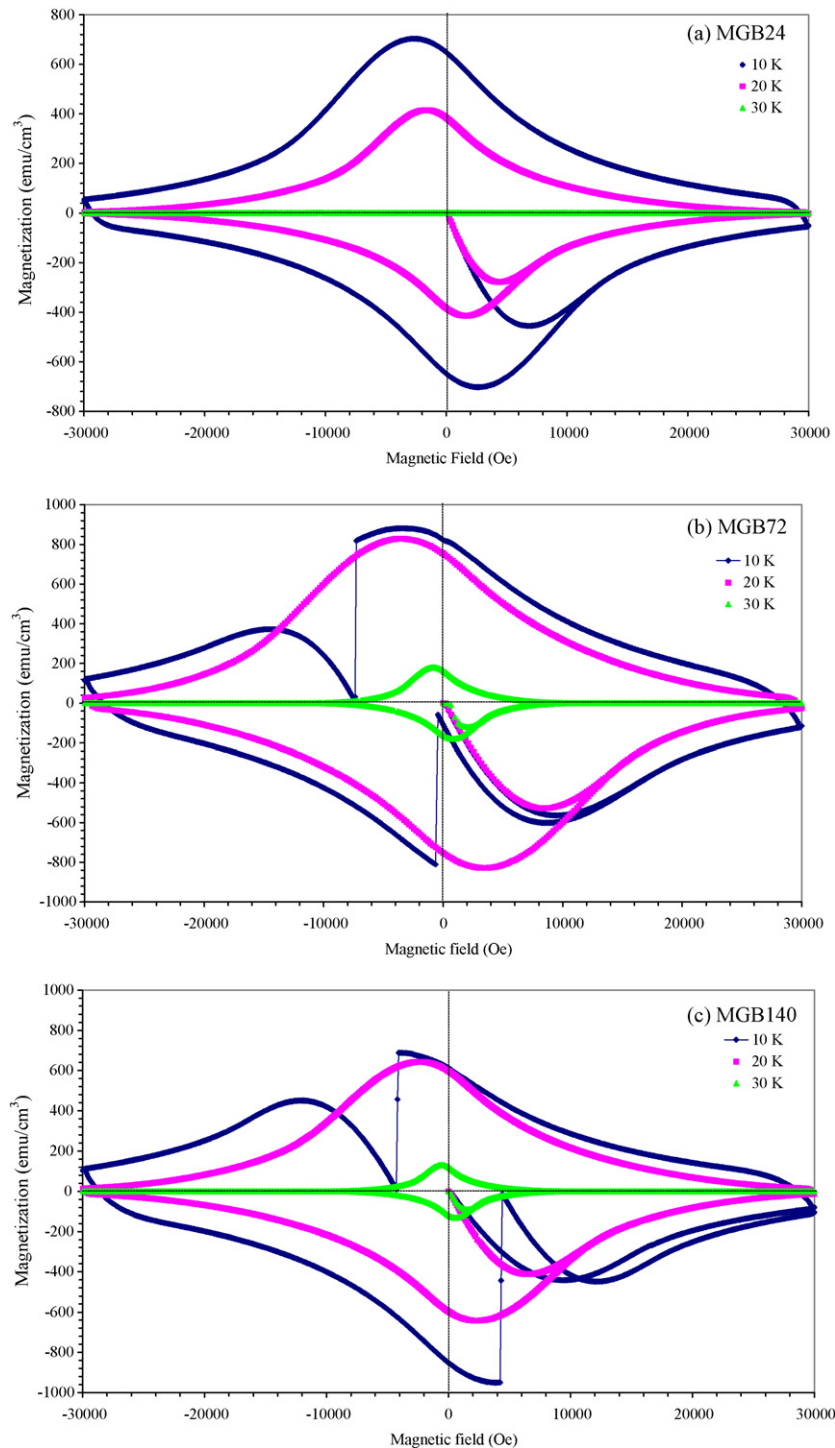


Fig. 4.  $M$ - $H$  loops of three samples measured at 10, 20 and 30 K.

make bulk  $\text{MgB}_2$ . Here after the samples will be referred as MGB24, MGB72 and MGB140.

Structural analyses were carried out in an X-ray diffractometer (XRD), Rigaku Dmax/III.  $\text{Cu K}\alpha$  radiation was used and X-rays were normally generated at 40 kV and 30 mA. Measurements were performed at  $2\theta$  between  $5^\circ$  and  $70^\circ$  with steps of  $0.02^\circ$ .

Analysis of the particle size of the powders was monitored by a high resolution JEOL 840F Scanning Electron Microscopy (SEM) working at 5 kV, and Energy Dispersive X-ray (EDX) analyses were performed using a JEOL 6300 SEM working at 10 kV. The superconducting transition temperature was determined by moment–temperature measurement and ac susceptibility measurement at temperatures between 10 K and 40 K using a Quantum Design Physical Properties Measurement system (PPMS). The magnetic properties ( $M$ – $H$  loops) of samples were determined using a Vibrating Sample Magnetometer (VSM) on the same system.

### 3. Results and discussion

The chemical reaction in the powder mixture during mechanical alloying for 24, 72, and 140 h was investigated by X-ray diffractometer. Fig. 1a shows the X-ray spectrums of powders milled for 140 h by a ball milling under nitrogen atmosphere. (The X-ray spectrum of samples MGB24 and MGB72 was not included here.) The diffraction patterns indicate that the main phase is residual unreacted Mg powders. No boron peak was observed in the X-ray diffraction pattern due to its amorphous structure. The 140 h milled powders sintered at  $650^\circ\text{C}$  for 30 min in a special designed atmosphere controlled furnace showed the phase formation of  $\text{MgB}_2$  together with some amounts of unreacted Mg and  $\text{MgO}$  phases as shown in Fig. 1b. As seen in Fig. 1c, which was heat treated at  $750^\circ\text{C}$  for 30 min, the main phase is  $\text{MgB}_2$  together with some amounts of unreacted Mg and  $\text{MgO}$ . As clearly seen from Fig. 1c, the intensity of the main peak belongs to  $\text{MgB}_2$  at around  $42^\circ$  decreased and broadened which is an indication of particle size reduction after milling process. Same phase formation was determined for 24 h and 72 h milled

and reacted powders (not included as a figure). It was reported [2] that nanocrystalline  $\text{MgB}_2$  was produced by mechanical alloying using Jar and balls made from tungsten carbide and the X-ray spectrum showed  $\text{MgB}_2$  main phase together with small peaks of Mg and WC (tungsten carbide). The decrease of the intensity of Bragg peaks and the increase of the full width at half maximum (FWHM) for the ball milled powders of  $\text{MgB}_2$  phase indicate that the crystallite size becomes smaller and the lattice strain was introduced by the mechanical milling.

Fig. 2 shows SEM images at different magnifications of powders MGB140. Images clearly indicate that the material mainly consists of spherical crystals and the crystalline sizes are much less than 100 nm and nanocrystalline grains are strongly agglomerated. The average crystalline size of powders should be different and the log time milled powders have got lowest particle size as normally expected. It is well known that a narrow size distribution and small-sized particles can be particularly effective for enhancing the reaction between Mg and B.

Fig. 3a shows the real and imaginary parts of ac susceptibility versus temperature for the samples MGB72 and MGB140. As seen from the curves, the superconducting onset transition temperatures were determined from the real parts of the ac susceptibility to be approximately 37 K and 36.5 K for the samples milled for 72 h and 140 h respectively which is the  $T_c$ 's less than the typical value of 39 K of the commercial  $\text{MgB}_2$  samples. Additionally, the lowest  $T_c$  was observed for the MGB140 sample. Consequently, mechanical alloying introduce defects in grains during the milling and these defects work as pinning centres and results in the suppression of the superconducting transition temperature. The superconducting transition temperatures of MGB24, MGB72 and MGB140 samples

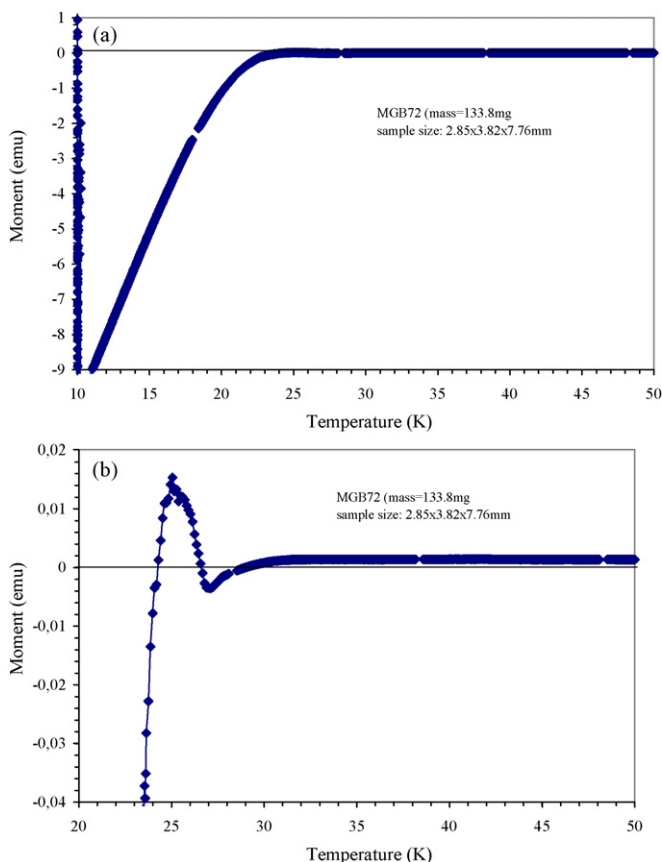


Fig. 5. Moment–temperature variation for MGB72 measured at 10 K.

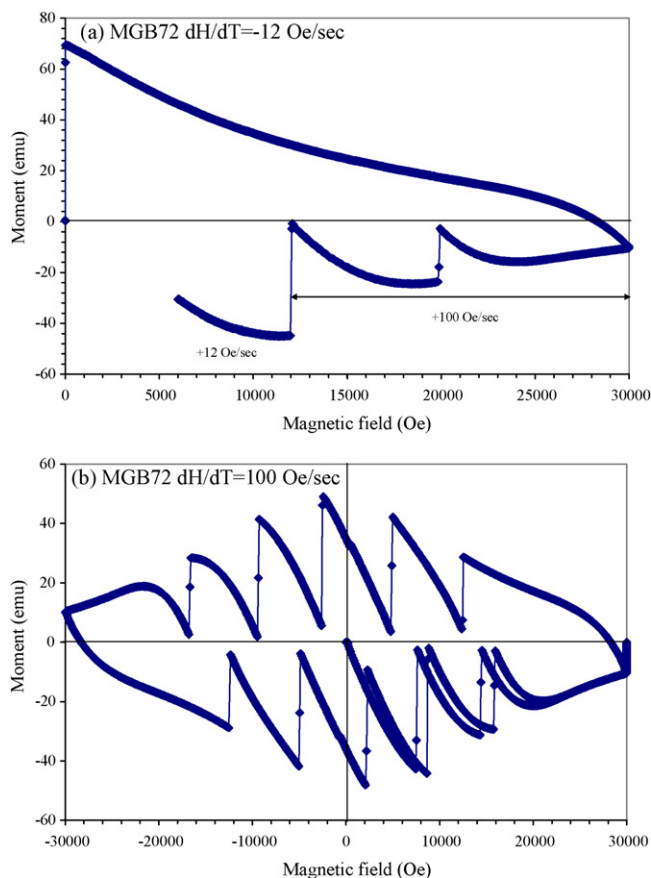


Fig. 6. (a)  $M$ – $H$  loops of MGB72 at different sweeping rate of magnetic field and (b) several flux jumps observed at the rate of 100 Oe/s.

were also determined by measuring the magnetization as a function of temperature as shown in Fig. 3b. It was found that the onset temperature of  $M(T)$  represents the off set temperature of ac susceptibility results. It was thought that long time milling caused the reduction of particle size in nano-scale, increases the number of pinning centres and induces residual strain in bulk samples which may be the origin of the reduction of  $T_c$ .

Fig. 4 shows the magnetization curves,  $M(H)$ , for samples MGB24, MGB72 and MGB140, which were measured at  $T = 10, 20$  and 30 K. As seen from the curves, there is symmetry in increasing and decreasing field branches, i.e.,  $M(H^+) \approx -M(H^-)$  was observed which means that the contribution of the equilibrium magnetization and the surface pinning is negligible compared to that of the bulk pinning [14]. It is well known that a flux jumping phenomenon has been a severe problem for the application of superconductors [9]. A thermal impulse occurs during the measurement and causes the decreasing of critical current density and allows flux to penetrate as an avalanches process. In our samples MGB72 and MGB140, a complete flux jumping was observed at the temperature of 10 K as shown in Fig. 4b and c respectively. The reason of flux jumping was given by Ref. [9] as since the magnetic diffusion rate becomes faster than thermal diffusion rate at low temperature, magnetic flux abruptly moves to cause flux jumps. In order to understand the jumping in curves as a flux jump, several experiments were performed on the sample MGB72 (mass = 133.8 mg)

at 10 K at Quantum Design, Inc., San Diego. Fig. 5a shows moment versus temperature of sample MGB72 and it is clearly seen that a noticeable amount of heating occurs ( $\sim 0.3$  K jumps at 10 K) at these jumps. This is a strong evidence for a real physical effect. Furthermore, heating is consistent with a sudden inrush of magnetic flux as the magnetic energy of flux expulsion (volume integral of  $B^2$ ) will be converted to thermal energy. In addition, a local jump was also observed at around 25 K as shown in Fig. 5b. It was determined that a low sweeping rate avoids these “avalanches”, allowing the field gradients to stay close enough to equilibrium so that the avalanche effect is not triggered. This is seen in the Fig. 6a no flux jump were observed after the sweep rate was reduced to 12 Oe/s. In contrast, 100 Oe/s leads to numerous jumps as shown in Fig. 6b. Consequently, the complete flux jumps were observed on the samples MGB72 and MGB140 at 10 K while no any flux jump for sample MGB24. The critical current density  $J_c$  (in  $\text{A cm}^{-2}$ ) of above indicated samples has been estimated by the extended Bean model with the equation:  $J_c = \frac{20 \Delta M}{L_1} \left(1 - \frac{L_1}{3L_2}\right)^{-1}$  where  $\Delta M$  (in  $\text{emu/cm}^3$ ) is the width of the hysteresis,  $L_1$  and  $L_2$  (both in cm) are sample dimensions perpendicular to the magnetic field with  $L_2 > L_1$ . As seen from Fig. 7, the values of  $J_c$  in zero field for sample MGB24 were calculated to be  $2 \times 10^2$  at 30 K,  $8.75 \times 10^4$  at 20 K and  $1.47 \times 10^5 \text{ A cm}^{-2}$  at 10 K. The  $J_c$  values were increased to  $3.67 \times 10^4$  at 30 K,  $1.38 \times 10^5$  at 20 K and  $1.7 \times 10^5 \text{ A cm}^{-2}$  at 10 K for sample MGB72. The highest critical current densities,  $J_c$ , were determined for sample MGB140 to be  $2.74 \times 10^4$  at 30 K,  $1.37 \times 10^5$  at 20 K and  $2.7 \times 10^5$  at 10 K. Therefore, it was pointed out that the samples showed an enhanced critical current density due to the improved pinning properties which are related to the milling time.

#### 4. Summary

High density nano-crystalline  $\text{MgB}_2$  bulk superconductors with induced pinning centres were prepared from elemental precursors by a sequence of ball milling, heat treatment, and final pressing. All samples showed transition temperature around 34 K from moment–temperature and 36–37 K from the ac. susceptibility measurements. The complete flux jump was observed at 10 K in  $\text{MgB}_2$  bulk samples, which were milled for 72 h and 140 h and sintered at 700 °C for 30 min. The critical current density,  $J_c$ , was enhanced by increasing milling time which can be attributed to increase of number of pinning centres.

#### References

- [1] J. Nagamatsu, N. Nakagawa, T. Muranaka, Y. Zenitani, J. Akimitsu, Nature 410 (2001) 63–64.
- [2] B. Lorentz, O. Perner, J. Eckert, C.W. Chu, Supercond. Sci. Technol. 19 (2006) 912–915.
- [3] O. Perner, W. Häßler, J. Eckert, C. Fischer, C. Mickel, G. Fuchs, B. Holzapfel, L. Schultz, Physica C 432 (2005) 15–24.
- [4] X.L. Wang, S.H. Zhou, M.J. Qin, P.R. Munroe, S. Soltanian, H.K. Lui, S.X. Dou, Physica C 385 (2003) 461.
- [5] Y.D. Gao, J. Ding, Q. Chen, G.V.S. Rao, B.V.R. Chowdari, Acta Mater. 52 (2004) 1534–1553.
- [6] A. Gumbel, J. Eckert, G. Fuchs, K. Nenkov, K.-H. Müller, L. Schultz, Appl. Phys. Lett. 80 (15) (2002) 2725–2727.
- [7] O. Perner, J. Eckert, W. Häßler, C. Fischer, J. Acker, T. Gemming, G. Fuchs, B. Holzapfel, L. Schultz, J. Appl. Phys. 97 (2005) 056105.
- [8] O. Perner, J. Eckert, W. Häßler, C. Fisher, K.-H. Müller, G. Fuchs, B. Holzapfel, L. Schultz, Supercond. Sci. Technol. 17 (2004) 1148–1153.
- [9] Y. Kimishima, S. Takami, T. Okuda, M. Uehara, T. Kuramoto, Y. Sugiyama, Physica C 463–465 (2007) 281–285.
- [10] R.G. Mints, Phys. Rev. B 53 (18) (1996) 12311–12317.
- [11] K. Chen, S.W. Hsu, T.L. Chen, S.D. Lan, W.H. Lee, P.T. Wu, Appl. Phys. Lett. 56 (1990) 2675.
- [12] A. Gerber, A. Milner, Phys. Rev. B 62 (2000) 9753.
- [13] T.H. Johansen, M. Baziljevich, D.V. Shantsev, P.E. Goa, Y.M. Galperin, W.N. Kang, H.J. Kim, E.M. Choi, M.-S. Kim, S.I. Lee, Eur. Phys. Lett. 59 (2002) 599.
- [14] C.U. Jung, S.-I. Lee, J. Magn. Magn. Mater. 310 (2007) 501–503.

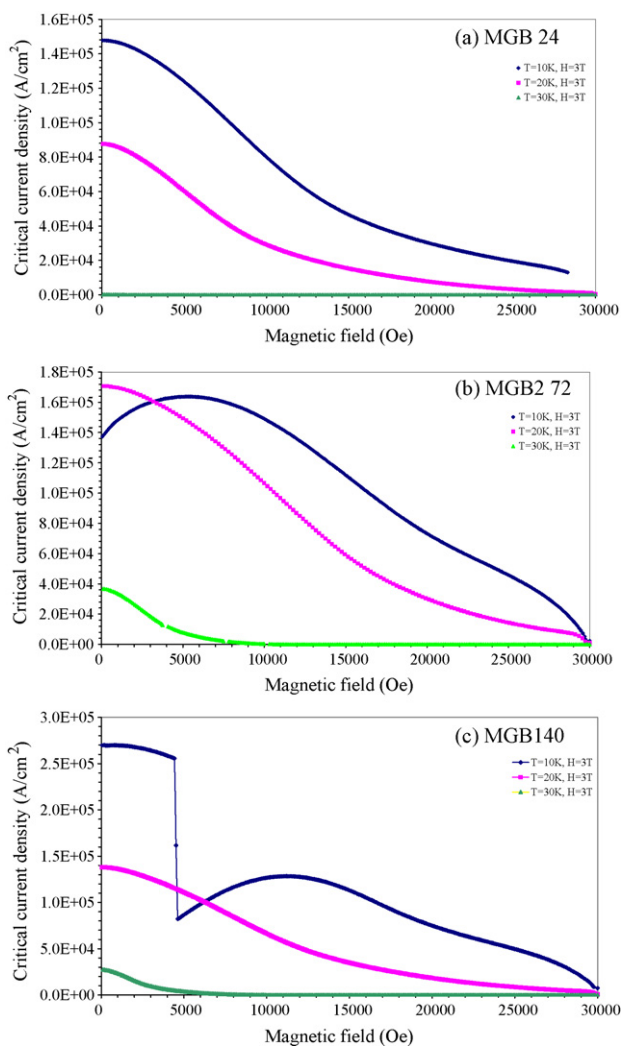


Fig. 7. Critical current density of three samples calculated from magnetization loops.